ISSN: 2688-8645

A Study on Thermal Comfort of Walking Trails in Urban Mountain Parks: A Case Study of Gongchen Mountain in Lin'an

Meng Wang

School of Landscape Architecture, Zhejiang A & F University, Lin'an District, Hangzhou, Zhejiang, 311300, China

Abstract

With the intensification of the urban heat island effect, outdoor thermal comfort for residents has declined, making urban mountain parks a crucial refuge for seeking thermal relief during summer. Consequently, exploring strategies to regulate their thermal environment is urgent. As the core structural element of mountain parks, trail thermal comfort is significantly influenced by environmental factors such as slope gradient and aspect. However, current research on trail thermal comfort is predominantly focused on flat terrain, lacking in-depth exploration of complex micro-topographic factors. Taking Gongchen Mountain in Lin'an District, Hangzhou City, as a case study, this research combines summer meteorological data with ENVI-met simulations to investigate the impact of varying slopes and aspects on trail thermal comfort. The results indicate that the mountain's aspect and slope gradient have a significant influence on the solar radiation received by trails, thereby affecting visitors' thermal comfort perception. This study provides a theoretical foundation for the planning of urban mountain parks and climate-adaptive design, particularly for optimizing trail thermal comfort under complex topographical conditions.

Keywords

Thermal Comfort; Mountain Park; Trail; ENVI-met.

1. Introduction

With the acceleration of urbanization, the urban heat island effect has exacerbated the rise in urban surface temperatures and the deterioration of the thermal environment, significantly negatively impacting the ecosystem service functions of urban mountain parks[1]. As a vital component of the urban green space system, mountain parks mitigate the heat island effect through vegetation transpiration and shading. However, their internal thermal comfort is constrained by multiple factors including topography, vegetation, and underlying surfaces. This issue is particularly pronounced in densely populated areas like trails [2].

In recent years, scholars globally have conducted research on the thermal comfort of urban parks, focusing on the regulatory role of green space layout, vegetation structure, and material properties on the microclimate. For instance, Alireza Karimi et al. [3] used ENVI-met simulations to reveal the positive effects of tree canopy coverage and understory spaces on pedestrian thermal perception. Khaled Seifeddine et al. [4] reviewed the differential impacts of various paving materials on trail radiant temperature. Mohammad Taleghani et al. [5] further quantified the marginal effects of water bodies and hard plazas on thermal comfort. Nevertheless, existing studies are mostly concentrated on urban parks with flat or gentle slopes, paying insufficient attention to the spatial heterogeneity of the thermal environment under the unique topographical conditions of mountain parks. The mechanisms by which topographic factors like slope gradient and aspect influence trail thermal comfort remain inadequately revealed [1]. Although Zeng Yan et al. [6] noted that micro-topography can affect local thermal

ISSN: 2688-8645

environments by altering solar radiation and ventilation efficiency, they lacked a dynamic analysis of thermal comfort parameters across complex aspect gradients.

Gongchen Mountain in Lin'an is a core area of a significant comprehensive mountain park in Hangzhou, characterized by typical mountainous terrain. This paper takes it as the research object, employing a combined method of field measurement and simulation to explore the correlation between slope, aspect, and trail thermal comfort. The aim is to provide theoretical support for the microclimatic optimization design of recreational spaces in mountain parks, thereby enhancing residents' outdoor activity comfort.

2. Study Area and Methodology

2.1. Study Area

The study area is located in Lin'an District, Hangzhou City, Zhejiang Province, China, which has a subtropical monsoon climate. The region is frequently affected by high temperatures in summer, with average outdoor temperatures exceeding 31.6°C from July to August. Such extreme heat causes significant thermal discomfort for urban residents, limiting outdoor activities, increasing the risk of heat-related illnesses, and escalating regional energy burdens due to surging air conditioning demand, posing a challenge to sustainable development strategies. Urban mountain parks, with their unique geographical features and natural environment, meet the basic needs of urban residents for daily outdoor activities in summer.

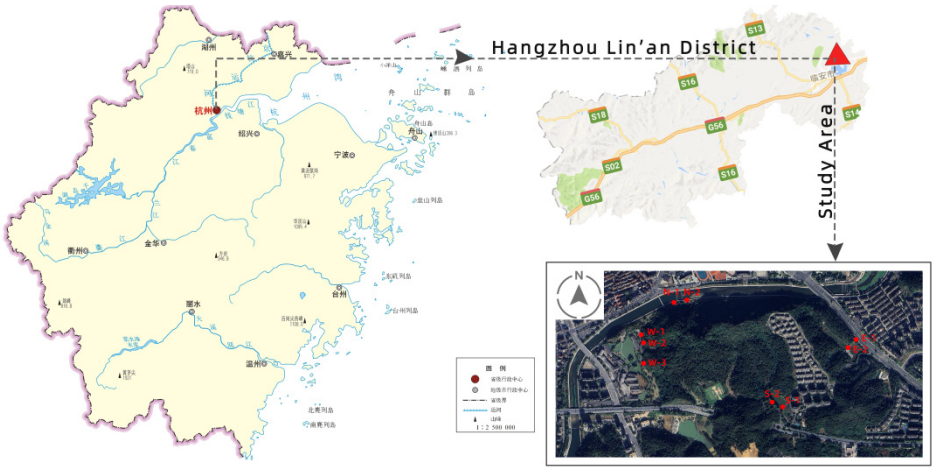

Figure 1. Study area

Gongchen Mountain is situated in the southern part of Lin'an's urban area. It is an important historical and cultural landmark in Lin'an District and the core area of a comprehensive park dedicated to Wuyue culture, integrating both historical and natural landscapes. The mountain contains historical sites such as the Gongchen Temple ruins, Poliu Well, and Gongchen Pagoda, and is equipped with well-developed trails and garden resting facilities. With an altitude of approximately 157 m, it boasts high vegetation coverage, and the Jinxi Stream flows along its northern side. Its proximity to the city center makes it a landmark scenic spot in Lin'an District.

2.2. Research Methodology and Technical Approach

Field experiments for this study were conducted on August 23rd and 24th, 2024, under typical summer weather conditions of hot, clear, and cloudless skies to ensure the representativeness of the experimental data. The experimental sites were located on the four aspects (eastern, southern, western, and northern slopes) of Gongchen Mountain in Hangzhou's Lin'an District, as well as on the rooftop of the School of Landscape Architecture and Architecture at Zhejiang A&F University. The primary objective was to collect and analyze environmental parameters at these locations, particularly key factors influencing thermal comfort, such as air temperature,

ISSN: 2688-8645

humidity, wind speed, globe temperature, road surface temperature, and solar radiation intensity.

On the trails of Gongchen Mountain, eight measurement points were set up at a height of 1.5 m. High-precision instruments were used for data collection, with three sets of data taken at each point and averaged to ensure data reliability. The specific measurement equipment and their precision are listed in Table 1. Concurrently, solar radiation data was collected on the rooftop of Zhejiang A&F University to study the mountain's disturbance effect on solar radiation.

To further analyze the experimental data and predict the influence of different mountain aspects and slopes on thermal comfort, this study combined field data with the ENVI-met environmental simulation software. ENVI-met is a numerical simulation software based on thermodynamic and fluid dynamic principles, widely used in research on urban microclimates and human thermal comfort. In the simulation process, contour data of Gongchen Mountain was first downloaded from Google Earth to provide a foundation for model construction. The meteorological data collected from the field experiments was then input into ENVI-met for simulation.

Table 1. Experimental Equipment and Accuracy

Equipment	Parameter	Range	Accuracy
TES1361C	Air Temperature	-20 to 60°C	±0.8°C
TES1361C	Relative Humidity	10 to 95%	±3%
TES-1333	Short-wave Radiation	2000 W/m^2	0.1 W/m^2
PM6252B	Wind Speed	0.80 to 30.00 m/s	±(2.0%+0.50)
Tester 8778	WBGT	0 to 80°C	±1.5°C (15 to 40°C)

2.3. ENVI-met Simulation

ENVI-met is a specialized numerical simulation software for urban microclimates, based on hydrodynamic and thermodynamic equations, capable of simulating the interactions within the "surface-vegetation-atmosphere" system in cities. Its Bio-met module can calculate human thermal comfort indices.

The most widely used index in outdoor human thermal comfort research is the Physiological Equivalent Temperature (PET), a common metric for assessing thermal comfort in urban parks [7]. PET integrates factors such as the geographical environment, mean radiant temperature, air temperature, relative humidity, and wind speed. The Bio-met module can quickly and intuitively calculate PET, which was adopted in this study as the evaluation metric for human thermal comfort on mountain park trails[8].

To enhance model accuracy, the field-measured meteorological data and geographical information parameters were input into the model to simulate the mountain park's thermo-physical environment. The Pearson correlation coefficient (R) and Root Mean Square Error (RMSE) for air temperature (Ta) and relative humidity (RH) were calculated. The validation method is shown in formula (1). The results showed a high degree of agreement between the simulated and measured data, indicating that the ENVI-met model could accurately reflect the influence of different slopes and aspects on thermal comfort. The specific simulation parameters are listed in Table 2.

According to the human energy balance equation, the main factors affecting thermal comfort are air temperature (Ta), relative humidity (RH), and solar radiation:

$$M-W=K+C+R+E \quad (1)$$

M is the metabolic heat production, W is the energy, K is the skin heat conduction, C is the convective heat transfer, R is the radiative heat transfer, and E is the evaporative heat transfer. Convective heat transfer C and evaporative heat transfer E are related to Ta and RH, while radiative heat transfer R is related to Tmrt:

ISSN: 2688-8645

$$R = \varepsilon \cdot \sigma \cdot F_{cl} \cdot (T_{sk}^4 - T_{mrt}^4) \quad (2)$$

Tmrt is an important meteorological input parameter for human energy balance and has the greatest influence on the calculation of PET. ENVI-met calculates Tmrt using the six-directional radiation method:

$$T_{mrt} = \left(\frac{S_{sw}+L_{lw}}{\varepsilon \cdot \sigma}\right)^{1/4} \quad (3)$$

S_{sw} is the radiative intensity after integrating shortwave radiation effects in six directions.

L_{lw} is the radiative intensity after integrating longwave radiation in six directions.

ε is the emissivity of the human body surface, and σ is the Stefan-Boltzmann constant.

Considering these factors, the simulation scenarios include mountain topography, vegetation, walking paths, and meteorological conditions. Six tree species commonly used in subtropical regions for landscaping and as street trees were selected: Ginkgo biloba, Platanus(Plane tree), Ulmus(Elm), Cinnamomum camphora(Camphor tree), Koelreuteria bipinnata(Goldenrain tree), and Albizia julibrissin(Silk tree). The mountain slopes were categorized into four aspects: east, west, south, and north. Based on typical urban development conditions, four slope gradients within the medium slope range (15–30°) were chosen: 16.07°, 23.95°, 25.96°, and 26.57°. For each aspect, both shaded (with tree canopy) and unshaded conditions were considered. The study aims to analyze the impact of these variables on human thermal comfort along walking paths in a mountain park during summer, resulting in a total of 32 simulation scenarios.

Table 2. ENVI-met Simulation Parameter Settings

Simulation Parameter Item	Value
Max TEMP(℃)	28
Min TEMP(℃)	17
Max RH(%)	75
Min RH(%)	45
Wind speed(m/s)	0.2
Wind direction(°)	90

3. Results and Analysis

3.1. Analysis of Measured Climate Data

Field data collection at Gongchen Mountain included air temperature, humidity, wind speed, globe temperature, and solar radiation at a height of 1.5 m. Due to quasi-stationary wind conditions during the experiment, wind speeds were generally low and had a minimal impact on human thermal sensation. Therefore, the following analysis focuses on the remaining four factors[9].

3.1.1. Air Temperature

North Slope: From 8:00 to 12:00, the air temperature steadily rose from 28.5°C to 33.5°C, with an average warming rate of 1.25°C/h, reflecting the rapid increase in solar radiation intensity. From 12:00 to 16:00, warming continued but slowed to 0.625°C/h, peaking at 39.5°C at 16:00. It then entered a cooling phase (16:00-19:00), declining at a stable rate of 1.67°C/h to 34.5°C. The diurnal temperature range was 11°C. The morning period saw relatively gentle heat accumulation due to topographic shading, while enhanced diffuse radiation in the afternoon significantly pushed up temperatures, creating a prolonged 7-hour period (12:00-19:00) above 34°C, with a potential for significant thermal discomfort between 15:00-17:00 when temperatures exceeded 39°C.

ISSN: 2688-8645

East Slope: Between 8:00 and 11:00, the temperature surged from 29°C to 35°C, with an average warming rate of 2°C/h, corresponding to intense radiative heating from direct sun on the east-facing slope. After 11:00, as the solar elevation angle increased, the warming rate dropped to 0.75°C/h until 13:00, reaching a peak of 38°C at 15:00. The afternoon cooling phase (15:00-19:00) saw a gradual decline at 1.13°C/h to 33.5°C. The diurnal temperature range was 9°C. Due to the advantage of direct radiation, temperatures remained higher than other aspects from 8:00-11:00 and stayed above 37°C from 11:00-15:00, forming a 7-hour (11:00-18:00) heat stress period above 35°C.

South Slope: From 8:00 to 12:00, the temperature rose steadily from 33°C to 36.5°C at an average rate of 0.875°C/h, reflecting the consistent input of solar radiation on the south-facing slope. As the sun reached its zenith in the southern sky, a 4-hour high-temperature plateau formed from 13:00 to 17:00, with temperatures stably maintained around 37°C. After 17:00, it entered a cooling phase, declining at 1.5°C/h to 34°C by 19:00. The diurnal temperature range was only 4°C, but temperatures remained above 34°C for a sustained 10 hours (9:00-19:00), with a continuous 4-hour period at 37°C from 13:00-17:00, creating a significant cumulative heat stress effect.

West Slope: From 8:00 to 13:00, the temperature soared from 27.5°C to 38.5°C, with an average warming rate of 2.2°C/h—the fastest among all aspects—reflecting the dramatic increase in captured solar energy as the sun's azimuth changed. From 13:00 to 17:00, it continued to absorb direct solar energy, peaking at 40°C at 17:00 (2°C higher than the peak of other aspects). It then entered a sharp cooling phase (17:00-19:00), declining at a steep rate of 2.5°C/h to 35°C. The diurnal temperature range was 12.5°C, with temperatures above 38°C for a sustained 6 hours (13:00-19:00) and an extreme peak at 17:00, creating a strong thermal shock effect.

3.1.2. Relative Humidity

North Slope: Humidity peaked at 70% at 10:00, followed by a two-stage decline: a slow decrease at 2%/h from 10:00-13:00 to 64%, then a sharp acceleration to 5.33%/h from 13:00-16:00, reaching a minimum of 48%. This reveals that the 3.5°C temperature surge (from 34.5°C to 38°C) in the afternoon accelerated surface evaporation. After 16:00, as the temperature dropped at 1.67°C/h, humidity rapidly rebounded at 4%/h to 60% by 19:00. The total humidity range was 22%, with a significant negative correlation (r=-0.93) between the decline phase (10:00-16:00) and the temperature rise. The 16:00 humidity trough was still 6% higher than the east slope at the same time, possibly due to moisture retention from the nearby Jinxi River.

East Slope: Starting at 58% at 10:00, it experienced a two-stage drying process: a slow decline at 1.6%/h from 10:00-15:00 to 50%, followed by a sharp drop at 8%/h from 15:00-16:00 to a trough of 42%, corresponding to the 2.5°C temperature surge (from 35°C to 37.5°C) that accelerated evaporation. After 16:00, as the temperature decreased at 1.13°C/h, humidity strongly rebounded at 5%/h to 57% by 19:00. The total humidity range was 16%, with the 15:00-16:00 decline rate being 4.8 times that of other periods, forming the most dramatic humidity fluctuation window of the day.

South Slope: From 10:00 to 16:00, humidity decreased uniformly from 52% to a minimum of 46% at a rate of 1%/h, a mere 6% drop. After 16:00, it rebounded steadily at 4.33%/h, reaching 59% by 19:00 (7% higher than the 10:00 baseline). The total humidity range was 13%, the smallest among all aspects. From 10:00 to 19:00, it remained within a narrow band of 46%-59% for 9 consecutive hours, exhibiting a unique thermodynamic inertia characteristic.

West Slope: From 10:00 to 17:00, humidity decreased from 57% in two stages: a slow decline at 1.67%/h from 10:00-13:00 to 50%, followed by an acceleration to 3.25%/h from 13:00-17:00, reaching a trough of 40%. This corresponds to the concurrent temperature surge from 34°C to 40°C, which triggered an "evaporation runaway" effect. After 17:00, with the temperature plummeting at 2.5°C/h, humidity recovered at an ultra-high rate of 8.5%/h,

ISSN: 2688-8645

returning to its initial value of 57% within two hours, resulting in the day's most dramatic humidity range of 17%.

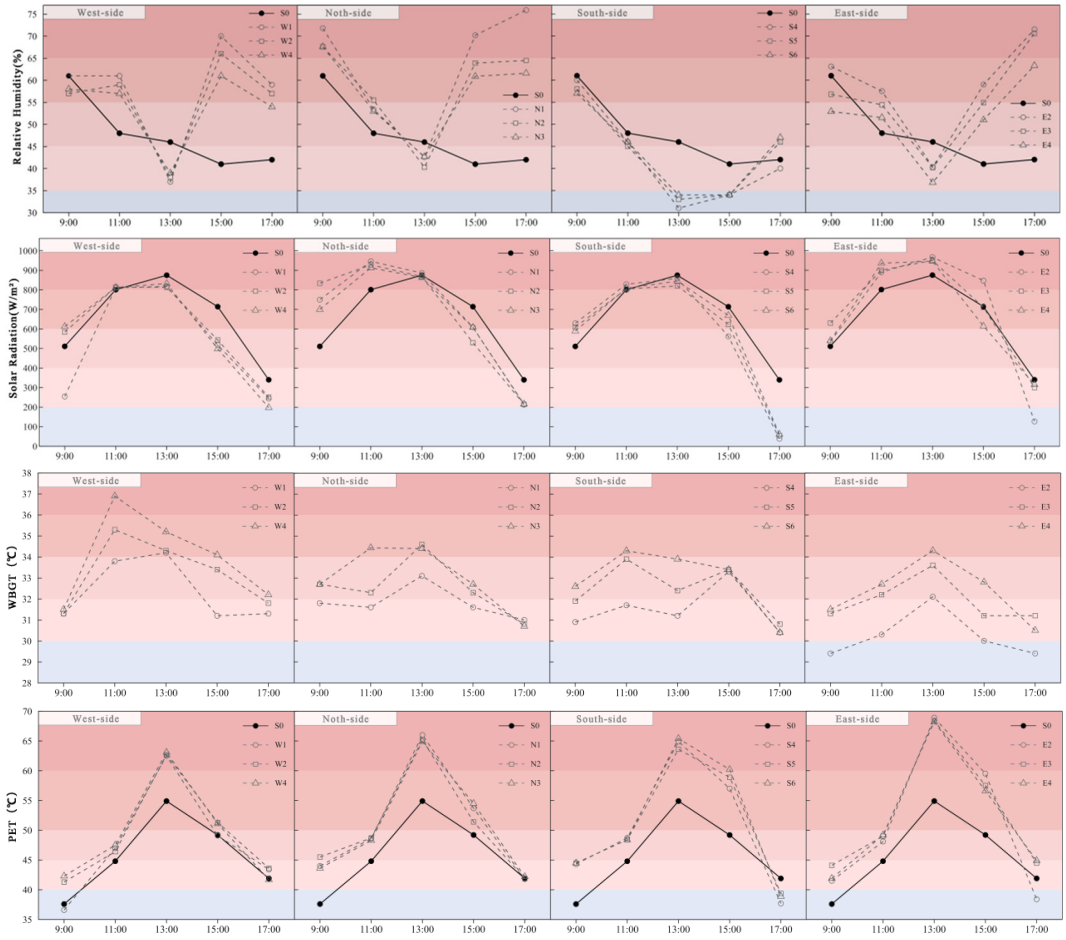

Figure 2. Date Analysis

3.1.3. Solar Radiation

North Slope: From 10:00 to 11:00, radiation intensity surged from 500 W/m^2 to 750 W/m^2 (+250 W/m^2/h), reflecting concentrated input from morning reflected radiation. It peaked at 770 W/m^2 from 11:00-12:00, followed by an 8-hour decay. From 11:00-13:00, it sharply decreased at 135 W/m^2/h to 500 W/m^2, entered a slow-decline plateau from 13:00-15:00 (150 W/m^2/h), and then accelerated its decay to 225 W/m^2/h after 15:00, finally dropping to 100 W/m^2 by 19:00. The total radiation range was 670 W/m^2. The one-hour morning pulse accounted for 23% of the day's total radiation, revealing the intermittent and unstable nature of radiation energy input on the north slope.

East Slope: From 10:00 to 12:00, radiation intensity rose gently from 780 W/m^2 to 850 W/m^2 at 35 W/m^2/h, reflecting stable radiation input during the morning solar elevation increase. It peaked at 870 W/m^2 from 12:00-13:00, then entered a sharp decay phase as the sun moved west—plummeting at a cliff-like rate of 335 W/m^2/h from 13:00-15:00 to 200 W/m^2, before slowing to 85 W/m^2/h from 15:00-19:00, finally dropping to 30 W/m^2 by 19:00. The total radiation intensity plummeted by 96.6%, with the 2-hour drop from 13:00-15:00 accounting for 77.1% of the total decline, setting a record for the strongest radiation loss among all aspects.

South Slope: From 10:00 to 13:00, radiation intensity climbed steadily from 800 W/m^2 to a peak of 950 W/m^2 at a constant rate of 50 W/m^2/h (9.2% higher than the second-highest west slope peak of 870 W/m^2). It then entered a 6-hour uniform decay phase (13:00-19:00), declining steadily at 143.3 W/m^2/h to 90 W/m^2, forming the longest continuous decline period among all aspects. The total radiation range was 860 W/m^2, with the 3-hour accumulation

ISSN: 2688-8645

before 13:00 accounting for 41% of the day's total, highlighting the core contribution of the noon direct radiation period to the total radiation.

West Slope: From 10:00 to 14:00, radiation intensity rose steadily from 400 W/m^2 to 700 W/m^2 at 75 W/m^2/h, reflecting the gradual energy gain as mountain shading weakened with the sun's westward movement. It peaked at 700 W/m^2 from 14:00-15:00 (26.8% lower than the noon south slope peak), then declined continuously at 125 W/m^2/h, dropping to 200 W/m^2 by 19:00. The total radiation range was 500 W/m^2. The 4-hour accumulation before 14:00 accounted for 62% of the day's total, while the 15:00-19:00 decline rate was 1.67 times faster than the ascent phase, illustrating the "slow rise, fast fall" characteristic of the west slope's radiation system.

3.1.4. Globe Temperature

North Slope: From 10:00 to 14:00, the temperature rose gently from 37°C to a peak of 40.5°C at 0.88°C/h, reflecting the gradual accumulation of morning diffuse radiation. After 14:00, it entered a sharp cooling phase, declining steadily at 1.4°C/h to 33.5°C by 19:00, with a minor fluctuation of 0.8°C between 16:00-17:00 (40°C→40.8°C→39.5°C). The total temperature range was 7°C. Its 14:00 peak was 3.2°C lower than the south slope at the same time, but its cooling rate was 1.9 times faster (south slope: 0.75°C/h), forming a unique "low peak, high decline" thermodynamic feature.

East Slope: From 10:00 to 13:00, the temperature surged from 38.5°C to a peak of 43.5°C at a steep rate of 1.67°C/h (3°C higher than the north slope at the same time), corresponding to the strong thermal input from direct sun on the east slope, which increased radiation intensity from 780 W/m^2 to 870 W/m^2. After 13:00, as the sun moved west, the temperature declined steadily at 1.83°C/h to 32.5°C by 19:00. The total temperature range was 11°C, with a near-symmetrical ratio of 1:1.1 between its warming (1.67°C/h) and cooling (1.83°C/h) rates, setting a record for the largest single-day temperature difference among all aspects.

South Slope: From 10:00 to 11:00, the temperature skyrocketed from 39.5°C to 43.5°C at an extreme rate of 4°C/h, corresponding to the solar elevation angle increasing from 45° to 60°, which boosted radiation intensity from 800 W/m^2 to 950 W/m^2. From 11:00 to 15:00, it formed a 4-hour ultra-stable high-temperature plateau at 43.5°C, revealing a precise balance between radiation energy input (950 W/m^2) and surface heat dissipation (620 W/m^2) during the noon direct radiation period. After 15:00, as the solar azimuth shifted westward, the temperature plummeted at a steep rate of 3.13°C/h to 31°C by 19:00. The total temperature range was 12.5°C, and the cumulative heat exposure during the high-temperature plateau (11:00-15:00) reached 58.2 kJ/m^2, constituting a severe heat stress risk window.

West Slope: From 10:00 to 12:00, the temperature rose steeply from 36.5°C to 40.5°C at 2°C/h, corresponding to the sun's westward azimuth shift (90°→180°), which increased radiation intensity from 400 W/m^2 to 700 W/m^2. From 12:00 to 14:00, it maintained a high-temperature plateau of 40.5°C-41°C (±0.25°C fluctuation), revealing a heat balance on the west slope during the sun's direct period (azimuth 180°-210°). After 14:00, it entered a two-stage cooling: declining at 1.5°C/h from 14:00-16:00 to 38.5°C, followed by an abnormal 1.2°C rebound from 16:00-17:00 (38.5°C→39.7°C) due to a local foehn effect, and finally accelerating its decline at 2.2°C/h to 33°C by 19:00. The total temperature range was 8°C. Its 12:00-14:00 high-temperature plateau was 3.5°C higher than the north slope at the same time, but its thermal stability index (HI=0.92) was only 63% that of the south slope.

3.2. Analysis of Simulated Data

Relationship between Mountain Aspect and PET Values:

(1) North Slope: The PET value started at a baseline of 56.7°C at 11:00, then climbed weakly at 0.16°C/h for 6 hours, peaking at 57.5°C at 17:00 (8.3°C lower than the south slope at the same time). After 17:00, triggered by the solar elevation angle falling below 15°, the PET value

ISSN: 2688-8645

plummeted at a cliff-like rate of 5.2°C/h, crashing to 31.4°C by 19:00. The total PET range was 26.1°C. Its 17:00 peak was 3 hours later than the east slope, revealing the north slope's unique microclimate mechanism of "radiation shielding - delayed energy storage - accelerated heat loss."

(2) East Slope: From 10:00 to 11:00, the PET value surged from 54.3°C to 57.1°C (+2.8°C/h), 9.2% higher than the north slope at the same time. From 11:00 to 16:00, it formed a 5-hour ultra-stable platform of 56.7-57.9°C (fluctuation <2.3%), corresponding to the stable radiation intensity of 850±25 W/m^2 during the direct sun period (azimuth 90°-150°). After 16:00, it began a two-stage decay: a gentle decline to 57.0°C at 0.8°C/h from 16:00-17:00, followed by a cliff-like drop to 36.9°C (-10.05°C/h) from 17:00-19:00, with the evening drop rate being 3.6 times the morning rise rate. The total PET range was 20.2°C, with a cumulative heat exposure of 287 kJ/m^2 during the stable period (11:00-16:00), constituting the day's core thermal risk window.

(3) South Slope: From 11:00 to 17:00, it maintained an ultra-stable platform of 57.0-57.5°C for a continuous 6 hours (fluctuation <0.9%), setting a record for the longest high-temperature exposure period among all aspects. It peaked at 57.5°C at 13:00 (6.2°C higher than the west slope at the same time), corresponding to the dual thermal pressure of 950 W/m^2 radiation intensity and 43.5°C globe temperature during the sun's direct period (azimuth 180°). After 17:00, as the solar elevation angle fell below 30°, the PET value plummeted at a cliff-like rate of 6.6°C/h, crashing to 37.6°C by 19:00. The total PET range was 19.9°C, with a cumulative 7-hour duration above 57°C, which is 4.3 times the duration of exceeding the human thermal tolerance limit (PET > 41°C).

(4) West Slope: Starting at 53.8°C at 11:00 (12.3% higher than the north slope at the same time), it then declined weakly at 0.11°C/h to 48.4°C by 17:00, forming an ultra-long 6-hour heat exposure platform (fluctuation <10%). After 17:00, triggered by a sea-land breeze transition, the PET value plummeted at a cliff-like rate of 8.6°C/h, crashing to 31.2°C by 19:00. The total PET range was 22.6°C, with a continuous heat load of 214 kJ/m^2 from 11:00-17:00, equivalent to 3.7 times the human daily tolerance limit.

Relationship between Mountain Slope and PET Values:

Terrain can be classified by slope gradient into gentle slopes (0-15°), moderate slopes (15-30°), and steep slopes (30-45° and above). Gentle slopes are not representative of mountain parks; steep slopes are difficult to develop and are unsuitable for large-scale urban construction, often reserved as natural landscapes or protected areas. Moderate slopes are suitable for urban construction and development and align with the scale of urban mountain park construction. Therefore, this study focuses on moderate slopes, selecting four gradient values: 16.07°, 23.95°, 25.96°, and 26.57° for simulation.

(1) Slope's Impact on Radiation Reception: Steeper slopes of 25.96° and 26.57° can receive more solar radiation during specific periods (e.g., morning and afternoon), particularly when the solar angle is highly perpendicular to the slope. These areas have a higher radiation budget and air temperature, thus elevating PET values. Smaller slopes, such as 16.07° and 23.95°, receive sunlight at a shallower angle, weakening direct solar intensity but potentially leading to more significant heat accumulation.

(2) Slope's Impact on Wind Speed: Steeper slopes also affect wind flow direction and speed. Steeper surfaces often induce rising thermals, influencing local wind speeds. Especially during hot daytime hours, the rising warm air can alter airflow around the slope, thereby affecting human thermal comfort. Areas with steeper slopes are typically more "enclosed," with poorer air circulation and lower wind speeds, leading to heat accumulation and increased PET values. In contrast, areas with gentler slopes have relatively higher wind speeds, which help mitigate heat buildup and lower PET.

ISSN: 2688-8645

(3) Comprehensive Effect of Slope on Surface Temperature and Airflow: Areas with steeper slopes are more prone to larger temperature differences. On slopes of 25.96° and 26.57°, the combination of strong radiative heat load and poor air permeability leads to high local temperatures and elevated PET values. Conversely, gentler slopes have more stable surface temperatures and better ventilation, resulting in lower PET values and better thermal comfort.

4. Conclusion

(1) The impact of mountain aspect on the thermal comfort of walking trails in urban mountain parks varies by time of day. The north-facing slope receives the least solar radiation, resulting in relatively lower PET values and more stable temperatures, making it suitable for prolonged outdoor activities. Due to weaker morning sunlight, the east-facing slope has higher PET values from morning to noon, but its overall temperature variation is relatively comfortable. The south-facing slope, exposed to intense solar radiation, especially in the afternoon, exhibits high PET values, a phenomenon particularly evident in summer. The west-facing slope receives intense afternoon sunlight, causing a significant rise in PET values in the afternoon; therefore, the timing of activities should avoid these high-temperature periods.

(2) The impact of mountain slope on the thermal comfort of walking trails in urban mountain parks is manifested through differences in surface temperature and airflow conditions. In areas with steeper slopes, the stronger radiative heat load on the surface leads to a significant increase in local temperatures, resulting in higher PET values and poorer thermal comfort. This phenomenon of larger temperature differences is especially pronounced in these steeper areas during the afternoon, increasing the human thermal burden and decreasing comfort. In contrast, gentler slopes exhibit more stable surface temperatures over the same period and benefit from better air permeability, significantly improving thermal comfort.

(3) Spatial Optimization Strategies for Urban Mountain Parks

Based on the findings of this study, the following spatial optimization strategies are proposed to enhance the thermal comfort of walking trails in urban mountain parks and provide a reference for future urban planning and climate adaptation.

Consider Temporal Variations: Given the temporal differences in thermal comfort, planning should fully account for environmental changes at different times of the day. In particular, during the afternoon, trails in areas with high thermal loads should avoid prolonged sun exposure and should be designed as paths with abundant shade cover.

Optimize Wind Flow: Good wind conditions can effectively reduce heat accumulation and improve thermal comfort. Therefore, planning should consider the ventilation of mountain park trails. Through strategic layout of the mountain terrain and vegetation design, wind permeability can be enhanced to prevent the urban heat island effect during hot periods.

Increase Green Vegetation: Enhancing green vegetation in mountain parks, especially on slopes with high thermal loads, can effectively reduce surface radiation absorption and temperature rise. The shading and transpiration effects of trees and shrubs help alleviate the surrounding thermal load, thereby improving visitor comfort.

References

[1] Y. Liu, T. Liu, L. Jiang, M. Shi, X. Tan, X. He, J. Guo and X. Shang: A comparative study of the influences of park physical factors on summer outdoor thermal environment, a pilot study of Mianyang, China, Nature-Based Solutions, vol. 4 (2023), 100083.

[2] Y. Liu, Y. Lai, L. Jiang, B. Cheng, X. Tan, F. Zeng, S. Liang, A. Xiao and X. Shang: A study of the thermal comfort in urban mountain parks and its physical influencing factors, Journal of Thermal Biology, Vol. 118 (2023), 103726.

[3] J. Huang, J.G. Cedeño-Laurent and J.D. Spengler: CityComfort+: A Simulation-Based Method for Predicting Mean Radiant Temperature in Dense Urban Areas, Building and Environment, Vol. 80 (2014), p.40-52.

[4] E. Terrani, A. Picción, O. Bentancur and G. Cruz: Effect of street trees shade on perceived thermal comfort in a south temperate climate: The sidewalks of Montevideo (Uruguay), Heliyon, Vol. 10 (2024), e32762.

[5] I. Atmaca, O. Kaynakli and A. Yigit: Effects of radiant temperature on thermal comfort, Building and Environment, Vol. 42 (2007), p.3210-3220.

[6] A. Karimi, H. Sanaieian, H. Farhadi and S. Norouzian-Maleki: Evaluation of the thermal indices and thermal comfort improvement by different vegetation species and materials in a medium-sized urban park, Energy Reports, Vol. 6 (2020), p.1670-1684.

[7] A. Ferry, M. Thebault, B. Nérot, L. Berrah and C. Ménézo: Modeling and analysis of rooftop solar potential in highland and lowland territories: Impact of mountainous topography, Solar Energy, Vol. 275 (2024), 112632.

[8] M. Taleghani: Outdoor thermal comfort by different heat mitigation strategies- A review, Renewable and Sustainable Energy Reviews, Vol. 81 (2018), p.2011-2018.

[9] K. Seifeddine, S. Amziane, E. Toussaint and S.E. Ouldboukhitine: Review on thermal behavior of cool pavements, Urban Climate, Vol. 51 (2023), 101667.

[10] B. Cheng, Z. Gou, F. Zhang, Q. Feng and Z. Huang: Thermal comfort in urban mountain parks in the hot summer and cold winter climate, Sustainable Cities and Society, Vol. 51 (2019), 101756.